Broadband dielectric study of oligomer of poly(vinyl acetate): A detailed comparison of dynamics with its polymer analog

Madhusudan Tyagi,[1,*] Angel Alegría,[2] and Juan Colmenero[1,2]
[1]*Donostia International Physics Center, Paseo Manuel de Lardizabal 4, 20018 San Sebastian, Spain*
[2]*Departamento de Física de Materiales, Universidad del País Vasco (UPV/EHU) and Unidad de Física de Materiales Centro Mixto (CSIC-UPV/EHU), Facultad de Química, Apartado 1072, 20080 San Sebastian, Spain*
(Received 1 December 2006; revised manuscript received 27 February 2007; published 18 June 2007)

We have studied the dynamics of a trimer of vinyl acetate (3VAc) using broadband dielectric spectroscopy over a wide temperature range to cover its primary and secondary relaxations. The dielectric spectra for the primary process over the entire temperature range have been described in terms of the Kohlraush-Williams-Watts approach [Williams and Watts, Trans. Faraday Soc. **66**, 80 (1970)]. The dielectric relaxation is found to show a characteristic crossover in the dynamics at 261 K through the temperature dependence of different dielectric parameters, viz., the relaxation time, shape parameter, and dielectric strength. Unlike in the polymer counterpart, this crossover temperature has been found to be different from the apparent merging temperature of the primary and secondary processes. Moreover, a direct comparison between the shape parameters in the case of 3VAc and poly(vinyl acetate) (PVAc) reflected a near absence of chain connectivity effects on the relaxation shape at the high-temperature side, which is interpreted as the decoupling of side group (containing the dipolar entity) motions from the main chain in the case of PVAc. A secondary relaxation for 3VAc was observed below its glass transition temperature, which is found to show the same activation energy as the β process in PVAc, for which new measurements have been made. However, their shapes showed different temperature dependences, which are discussed in terms of the molecular structure.

DOI: 10.1103/PhysRevE.75.061805 PACS number(s): 64.70.Pf, 77.22.Gm, 82.35.Lr

I. INTRODUCTION

When a liquid is cooled fast enough to avoid crystallization, the characteristic time of the primary relaxation process (the so-called α process) increases rapidly until it gets arrested at the glass transition temperature T_g (usually measured by differential scanning calorimetry), where the time scale of the relaxation becomes of the order of the experimental time scale ($\approx$100 s) [1]. The dynamics of this process in simple glass formers is characterized by some general features. The temperature dependence of relaxation rates is found to be of non-Arrhenius type and is usually described in terms of the well-known Vogel-Fulcher-Tammann (VFT) equation [2]. The corresponding spectral shape is found to be of non-Debye type (with monohydroxy alcohols as an exception [3]). In addition, quite often the dynamics of simple glass formers is found to exhibit a characteristic crossover at a temperature T_B, which usually falls in the temperature range $T/T_g=1.2-1.3$. This dynamic crossover is usually revealed as a change in the temperature dependence of the relaxation times, which can be assessed if relaxation times are measured sufficiently closely over a large temperature range with precise accuracy [4]. In general, most of these features displayed by simple glass formers are also shared by glass-forming polymeric systems, which also exhibit strongly non-Arrhenius dynamics and whose relaxation rates follow the VFT equation. The corresponding spectral shapes are also found to be strongly non-Debye type and, phenomenologically, are described rather well in terms of the Kohlrausch-Willimas-Watts (KWW) [5] relaxation function as in the case of simple glass formers. The dynamic crossover in polymeric systems has not been explored as a general feature, although some polymers exhibit a characteristic crossover in their dynamics. However, polymeric systems also exhibit a series of different characteristics which, in principle, should be related to their macromolecular chain connectivity. For instance, in polymeric systems the KWW shape parameter β_{KWW} shows rather lower values in comparison to low-molecular-weight (LMW) glass formers [2,6]. In addition, the temperature dependence of β_{KWW} is found to be weaker and its high-temperature limiting value is, usually, in the range 0.5–0.6.

In the literature, the study of oligomers and the corresponding polymers has mainly been devoted to finding the effects of chain connectivity on the separation of α and β processes [7–9]. It is been observed that, as the chain length increases, the separation between the two processes also increases. This is usually done by analyzing relaxation rates as a function of chain length. The chain connectivity effects on the shape of α and β processes, which should provide further insight into the molecular dynamics, is seldom studied. In addition, the effects of chain connectivity on the dynamic crossover and other dielectric properties such as dielectric strength has not been done so far. Therefore, a detailed dielectric study of how the dielectric properties discussed above are affected by chain connectivity is still lacking. In this paper, we would like to focus our attention on these topics. The polymer chosen for this comparison is the well-known poly(vinyl acetete) (PVAc), and we have compared its dielectric relaxation with that of its trimer (3VAc), above and below T_g. To observe the effects of chain connectivity, a detailed dielectric study of different oligomers with the polymer would be of the greatest advantage. Unfortunately,

*Email address: swxtytym@ehu.es

preparation of oligomers of different lengths of vinyl acetate is a challenge to chemists, and only the monomer and trimer can be synthesized with great effort. However, vinyl acetate is highly crystalline and cannot be measured in a fully amorphous state. Therefore, we took this opportunity and made a detailed comparison of the dielectric relaxation between the polymer and its only LMW amorphous counterpart. The primary relaxation in PVAc (T_g=314 K) has been known since as far back as the early 1940s [10] and has been a matter of continuous investigation thereafter [6,11,12]. Measurements on PVAc by combining broadband dielectric spectroscopy over an extremely large range of temperature and frequency with quasielastic neutron scattering were reported by us recently [13]. Thus, it is possible to compare our new measurements on 3VAc and observe the effects of chain connectivity on the polymer dynamics. In addition to the dynamic characteristics of the supercooled liquid, we will also investigate the β relaxation [10] observed below T_g. The origin of this β process in PVAc is still a topic of debate in the literature, as some authors attribute it to purely localized motions, while others advocate the idea that localized motions could be accompanied by some fluctuations within the main chain. The trimer studied here would be of particular interest in view of the above-mentioned results, and its study should allow a better and clearer insight into the molecular mechanisms involved in secondary relaxations.

The paper is organized in the following way. In the experimental section, we outline various experimental aspects concerning the samples and dielectric measurements. The next section is devoted to the tools of data evaluation for our dielectric measurements. The basic results obtained are presented in Sec. IV. In Sec. V, results obtained on both 3VAc and PVAc are discussed. In the last section we conclude our experimental findings.

II. EXPERIMENTAL SECTION

The oligomer investigated in this study is a trimer of vinyl acetate (3VAc) with the chemical formula H-CH_2-CH ($OCOCH_3$) -CH_2-CH($OCOCH_3$)-CH_2-CH($OCOCH_3$)-CH_3. The sample was synthesized by Polymer Source, Inc., Canada, starting from diacetyl acetone and followed by hydrogenation and acetylation [14,15]. Before the measurements, the sample was put in a vacuum oven at 313 K overnight to remove any traces of solvents. The sample was characterized by a glass transition at 209 K by conventional differential scanning calorimetry. In addition, a sample of PVAc, i.e., its polymer counterpart, was also measured for direct comparison. The PVAc sample used had a molecular weight of 83 kg/mol with a polydispersity of $\overline{M_w}/\overline{M_n} \approx 4.2$ (the same sample as used in Ref. [13]). Before the measurements, the PVAc sample was put in a vacuum oven at 400 K overnight to remove any trace of moisture, as it is known to affect the dielectric relaxation of PVAc.

Dielectric measurements on 3VAc above its T_g were performed in a wide frequency range of 10 mHz–20 GHz using three different experimental setups depending upon the frequency range. In the frequency range of 10^{-2}–10^7 Hz, dielectric measurements were made using a high-resolution Alpha dielectric analyzer supplied by Novocontrol, GmbH. For the frequency range of 10^6–10^9 Hz, an Agilent impedance analyzer HP4291B was used. For both setups, samples were prepared between two gold-plated electrodes of 30 and 10 mm diameter, respectively. Teflon spacers of 0.1 mm thickness and negligible area were used to maintain the constant distance between the two electrodes. For both setups, isothermal frequency measurements were carried out on a series of temperatures with a temperature stability better than 0.05 K. To extend the frequency range up to 20 GHz, the measurements were carried out in the frequency range of 200 MHz–20 GHz using an integrated system of an HP8361A vector network analyzer and dielectric probe kit HP85070E with an open ended coaxial probe. Complex permittivities were recorded using software supplied with the dielectric probe kit, which controls the vector analyzer for dielectric measurements. More details about the setups, related accuracies, and calibration of the instruments can be found elsewhere [13]. The β relaxation in 3VAc was also measured below its T_g in the frequency range 10^{-2}–10^7 Hz using the Alpha analyzer. As mentioned above, we have also carried out dielectric measurements on PVAc. The β relaxation of the PVAc sample was measured at a series of temperatures in the temperature range between 140 and 300 K using the Alpha analyzer.

III. DATA EVALUATION

In general, the main part of the α relaxation can be well described by the Kohlrausch-Williams-Watts [5] relaxation function in the time domain, which has a single shape parameter, and can be written as

$$\phi_{KWW}(t) = \exp\left[-\left(\frac{t}{\tau_{KWW}}\right)^{\beta_{KWW}}\right], \tag{1}$$

where β_{KWW} is the shape parameter defining the non-Debye nature of the relaxation and τ_{KWW} is the characteristic time. In the frequency domain, experimental dielectric results are usually described in terms of the empirical Havriliak-Negami (HN) relaxation function as [16]

$$\epsilon^* = \epsilon_\infty + \Delta\epsilon \frac{1}{[1+(i\omega\tau_{HN})^\alpha]^\gamma}, \tag{2}$$

where α and γ are two shape parameters ranging between 0 and 1 and τ_{HN} is the characteristic relaxation time. In addition, a purely conductive term $-i\sigma\omega^{-1}$ is usually added to Eq. (2) in order to account for the contribution of conductivity to the dielectric losses. Alvarez *et al.* [17,18] showed that the HN equation has one-to-one correspondence with the KWW equation in the time domain if the fitting parameters of the HN equation are restricted according to the following equation:

$$\gamma = 1 - 0.812(1-\alpha)^{0.387}. \tag{3}$$

Then

$$\beta_{KWW} = (\alpha\gamma)^{0.813}. \tag{4}$$

Therefore, Eq. (2) was used to fit the real and imaginary parts of the complex permittivity with the HN function with

a single independent shape parameter α. The result of such fitting is a full set of limiting frequency dielectric constants ϵ_0 and ϵ_∞ along with α and τ_{HN}. From α the equivalent values of β_{KWW} were calculated using Eq. (4) to facilitate comparison with literature data. The relaxation time corresponding to maximal loss, τ_m, was calculated as follows (2):

$$\tau_m = \tau_{HN}\left(\sin\frac{\alpha\pi}{2+2\gamma}\right)^{-1/\alpha}\left(\sin\frac{\alpha\gamma\pi}{2+2\gamma}\right)^{1/\alpha}, \tag{5}$$

which is essentially independent of any fitting procedure.

On the other hand, the secondary process found below T_g is usually symmetric and could be described well using the Cole-Cole (CC) equation which is a special case of the HN equation with parameter $\gamma=1$ ($\alpha\equiv\alpha_{CC}$). In this case, Eq. (6) yields $\tau_m=\tau_{HN}\equiv\tau_{CC}$. The relaxation times, then, can be calculated directly, and the values are very weakly affected by the uncertainties in spectral shape which are given in terms of the parameter α_{CC}. The temperature dependence of the corresponding relaxation times usually follows a thermally activated Arrhenius temperature dependence, i.e.,

$$\tau_m = \tau_{0,\beta}\exp\left(\frac{E}{RT}\right), \tag{6}$$

where $\tau_{0,\beta}$ is a preexponential factor usually of the order of the vibrational time, E is the activation energy, and R is the universal gas constant. Note that the CC shape parameter can be used directly to calculate the broadening of the log-normal distribution of relaxation times (see the following sections) which is considered to be a more appropriate way to describe thermally activated processes.

IV. RESULTS

A. Results on 3VAc

Figure 1 shows the general dielectric behavior of the α process in 3VAc at a series of temperatures to cover the entire range from its T_g up to 360 K (just about 20 K below its boiling point) along with the fits described above. As observed usually in a dielectric study, the frequency f_m at which ϵ'' takes the maximum value shifts to higher frequency with increasing temperature [Fig. 1(b)] which mainly shows the increasing mobility of molecules at higher temperatures. The maximum value of ϵ'' slightly decreases with increasing temperature as commonly observed for most of the glass-forming liquids. The dielectric relaxation of 3VAc in a comparatively low and limited frequency range (23 Hz–1 MHz) has been reported by Ikada *et al.* [15]; the results agree well with our measurements in the overlapping frequency and temperature range. A steep increase in the ϵ'' curves at lower frequencies [Fig. 1(b)] has been observed, which could be attributed to a purely dc conductivity contribution that varies inversely with the applied frequency. The increase at low frequencies is not found in the real part of the complex permittivity [Fig. 1(a)] indicating a purely Ohmic character of the conductivity. The fitting curves show some deviations from the experimental data at higher frequencies. These high-frequency deviations are a common phenomenon of LMW glass formers and polymeric systems [19]. These high-frequency deviations may also have some contribution from the β relaxation observed below T_g, which is shown in Fig. 2. This figure shows the dielectric relaxation loss spectra at different temperatures ranging between 140 and 196 K. As can be noted from Fig. 2, the maximum value of ϵ'' increases with increasing temperature. As we will see in the following sections, this indicates that the dielectric strength of the β process increases smoothly with increasing temperature. It can also be observed without any data analysis that, as usual, the β-relaxation spectra are much broader and symmetric in comparison to the α process observed above T_g.

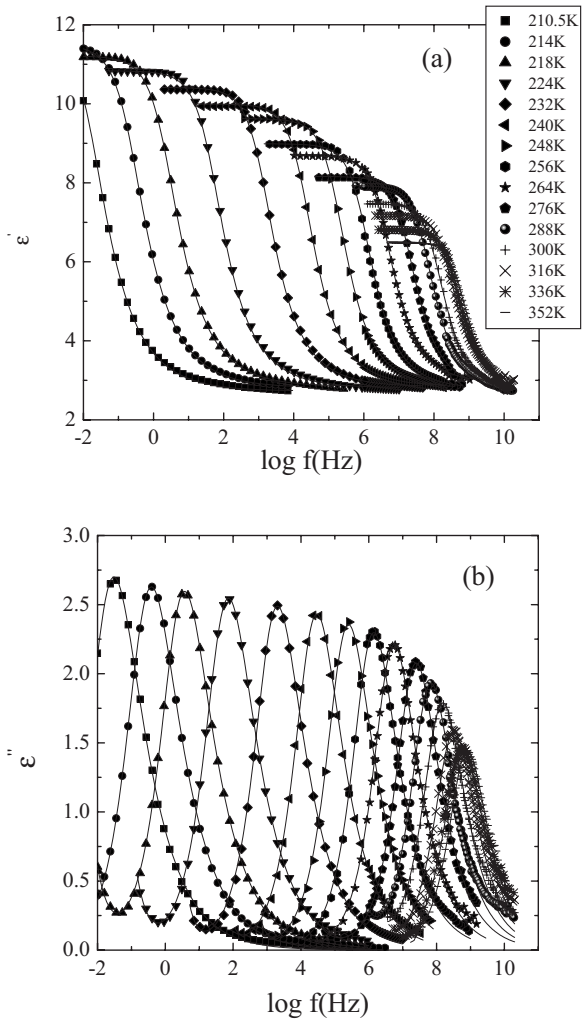

FIG. 1. Frequency dependence of (a) dielectric constant ϵ' and (b) dielectric loss factor ϵ'' for 3VAc at a series of temperatures between 210.5 and 352 K mentioned in (a) {plotted against $\log_{10}[f(\mathrm{Hz})]$}. The solid lines are fits corresponding to the KWW approach described in the text.

B. β relaxation in PVAc

The dielectric measurements on the β process of PVAc are shown in Fig. 3. At low frequencies, a slow rise in dielectric loss can be seen as the temperature increases toward T_g of PVAc. This is most likely the high-frequency tail of the α process, which is present at much lower frequencies at

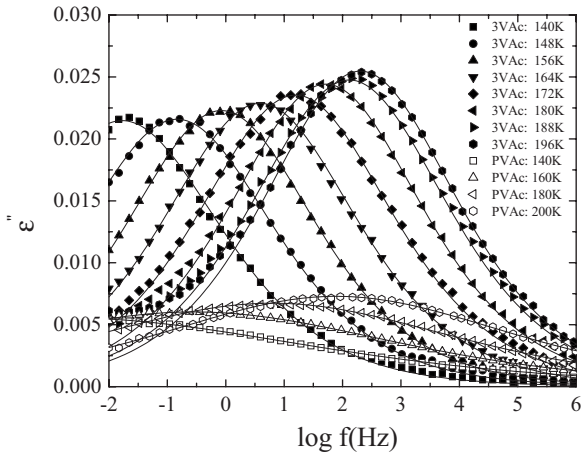

FIG. 2. Frequency dependence of dielectric loss factor ϵ'' of β relaxation for 3VAc in the temperature range between 140 and 196 K (filled symbols) {plotted against $\log_{10}[f(\mathrm{Hz})]$}. The solid lines are the fits corresponding to the Cole-Cole approach as discussed in the text. For the sake of comparison, the β process of PVAc at four temperatures, namely, 140, 160, 180, and 200 K is also shown by open symbols. The solid lines through the data points correspond to the combined fitting of the actual β process and the high-frequency tail of the α process in PVAc.

these temperatures, and is more than two orders of magnitude stronger than the β process under observation. As expected, a faster rise in the losses can be seen when approaching T_g, as a consequence of increasing peak loss frequency of the α process and, therefore, entering into the measured frequency window near T_g. This high-frequency tail can be approximately accounted for with a power law as follows:

$$\epsilon^* = (\epsilon_\infty + A\omega^{-\lambda}) + iB\omega^{-\lambda}, \tag{7}$$

where ϵ_∞ is the permittivity in the high-frequency limit of the α relaxation. The parameter λ, which influences the rise at

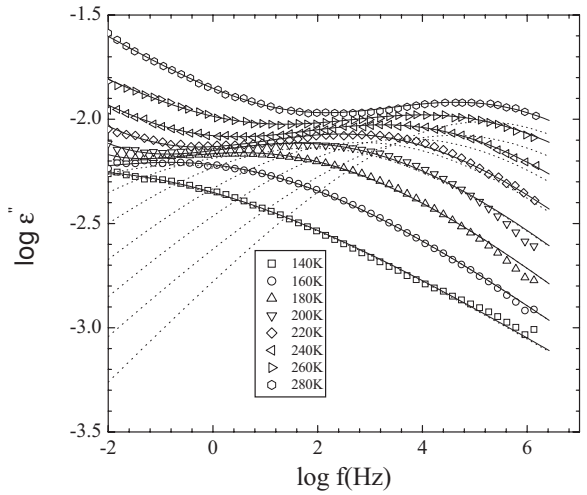

FIG. 3. Dielectric loss curves of β-process of PVAc in the temperature range 140–280 K in double logarithmic {$\log_{10}\epsilon''$ vs $\log_{10}[f(\mathrm{Hz})]$} plot. The rise at the low-frequency side with increasing temperature is caused by the high-frequency tail of the α relaxation. After subtracting the contribution of the high-frequency tail, the resulting curves for the β process are shown by dotted lines.

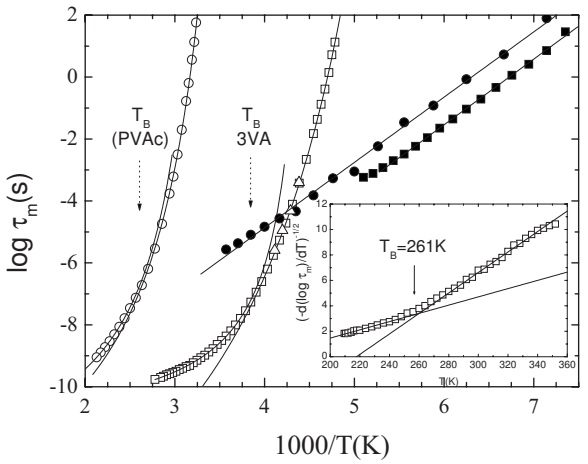

FIG. 4. Relaxation times of α process in 3VAc sample are shown by empty squares. The two VFTs are shown by solid lines, details of which are given in the text. For the purpose of comparison, relaxation times taken from Ref. [15] have also been added (open triangles). The relaxation times of the β process in 3VAc are shown by filled squares. For comparison, the α-relaxation data of PVAc (open circles) taken from Ref. [13] has also been added. The corresponding relaxation times for the β process are shown by filled circles (this work). The solid lines through data points correspond to the Arrhenius equation. The inset shows the plot of $[-d(\log_{10}\tau_m)/dT]^{-0.5}$ against temperature. The crossover temperature is the intersection of two solid lines which correspond to two VFTs shown in this figure.

lower frequency most, increases slowly from 0.18 until 0.3 in the temperature range 140–250 K. Above 250 K, the increase is sharper, indicating a faster rise of the tail of the α process in our frequency window. In this way, the high-frequency tail of the relaxation can be accounted for reasonably well in both the real and imaginary parts of the complex permittivity. The fits in Fig. 3 are a combination of this high-frequency tail and the Cole-Cole equation described in Sec. III. This resolved β process for PVAc is shown in Fig. 3 by dashed lines. Some of these curves were also shown in Fig. 2 for a direct comparison with the short-chain analog. One can see without any data analysis that the β process in PVAc is much broader in comparison to the secondary process in 3VAc.

V. DISCUSSION

A. α process

Figure 4 shows the relaxation times of the α process observed for 3VAc. Generally, the non-Arrhenius temperature dependence of the α process is well described by the Vogel-Fulcher-Tammann [2] equation

$$\tau(T) = \tau_0 \exp\left(\frac{DT_0}{T - T_0}\right). \tag{8}$$

In the above equation, T_0 is the temperature below T_g at which the extrapolated relaxation time tends to diverge, D is a parameter that can be related to the fragility concept first introduced by Angell [20], and τ_0 is of the order of the re-

ciprocal of the attempt frequency. A close description of the temperature dependence of relaxation rates using the VFT law has promoted various theoretical approaches like the free volume model [21] and the Adam-Gibbs theory [22] of cooperatively rearranging regions, because the VFT law can be deduced from these approaches. In the 3VAc sample, deviations from the VFT equation are strong, as a fit to a single VFT law does not describe the T dependence of the relaxation times satisfactorily over the entire temperature range employed here. For a critical examination of the validity of a single VFT law and in order to find the temperature regimes for different VFTs, a derivative method was proposed by Stickel *et al.*[4] according to which the derivative of the VFT equation with respect to temperature can be taken as

$$\left(\frac{\partial\{-\ln[\tau(T)]\}}{\partial T}\right)^{-1/2} = \frac{T - T_0}{(DT_0)^{1/2}}. \tag{9}$$

Accordingly, plotting the experimental data using Eq. (9) would result in linearity if a single VFT law were followed by the relaxation times over the entire temperature range. The slope and intercept of the straight line can be used to calculate back the corresponding VFT law (only the preexponent τ_0 remains free). The results of such an analysis are shown in the inset of Fig. 4, where it can be seen that to cover the entire temperature range studied here two VFT laws are required. The details of these obtained VFTs are as follows: (1) low-T VFT (T range 208–246 K); $\log \tau_0 = -16.4$, $D=14.2$, and $T_0=154.8$ K; (2) high-T VFT (T range 274–348 K); $\log \tau_0=-10.9$, $D=1.6$, and $T_0=217.7$ K. These VFT fits can be seen in Fig. 4. A characteristic crossover temperature T_B [4] can then be defined by the intersection of the two VFT laws where usually T_B is found to be in the range $(1.2-1.3)T_g$. As can be seen in the inset of Fig. 4, the value of T_B found in our measurements is 261 K which falls well within the above-mentioned range. Here, we would like to mention that there is no standard definition of T_B and hence, in the literature, authors usually refer to a narrow crossover region around T_B. For the purpose of comparison, the relaxation times of PVAc taken from Ref. [13] have also been added in Fig. 4, which also show strong departure from Arrhenius behavior. A crossover temperature of 387 K was obtained for PVAc. A quick comparison of T_B values in the two cases with their respective T_g's indicates that the dynamic crossover essentially occurs at the same temperature ($T_B=1.26T_g$) when normalized to the corresponding T_g. It has also been noted by some authors [23] that the deviations from a single VFT law can also be realized in terms of the ratio of the product of VFT parameters DT_0 for the low-T and high-T VFT laws, respectively. As this ratio increases, the deviations from the single VFT law becomes more and more apparent, e.g., in the case of *o*-terphenyl and salol [2,24]. In 3VAc, this ratio is close to 6.3 and hence the deviations are rather strong. This ratio is found to be close to 1.6 in the case of PVAc [25] and hence the deviation from a single VFT seems to be subtle. Therefore, the chain connectivity in the polymer seems to make the dynamic crossover weaker, although the crossover temperature with respect to T_g remains the same.

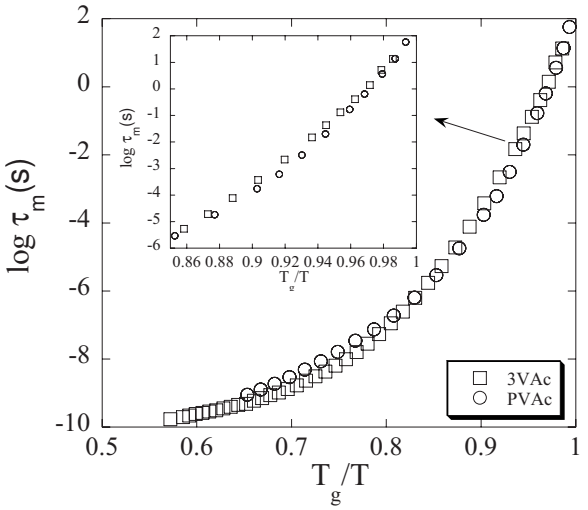

FIG. 5. Characteristic times for 3VAc and PVAc plotted against T_g/T. The inset is the magnified scale of the plot in the vicinity of $T_g/T=1$.

Another interesting aspect of this figure is the apparent merging temperatures of α and β processes in the two systems. In the case of PVAc, the merging temperature $T_{\alpha,\beta}$ seems to coincide with the crossover temperature T_B, while in the case of 3VAc the crossover temperature is much higher than the apparent $T_{\alpha,\beta}$ ($\approx$235 K). If the temperatures are normalized to their respective T_g's, it is observed that in the case of PVAc, the merging between the α and β processes occurs at relatively higher temperature than 3VAc. This seems to support the idea of an increasing $T_{\alpha,\beta}/T_g$ with growing molecular complexity as the molecular weight increases, as proposed in Ref. [7].

On the other hand, the glass-forming liquids could be categorized [20] as strong or fragile patterns depending upon deviations in their T dependence from Arrhenius behavior. A quick comparison between the fragilities of 3VAc and PVAc can be made by comparing the relaxation times when plotted against the normalized temperatures as shown in Fig. 5. This figure shows that the dynamics of PVAc exhibits slightly higher fragility according to the above-mentioned criterion. A convenient and quantitative measure of the fragility of the molecular system can be obtained by focusing on the long-time relaxation time end of the strong or fragile pattern. This can be done readily by calculating the slope of the relaxation rates at T_g when plotted against the normalized temperature as [26]

$$m = \left(\frac{d(\log \tau)}{d(T_g/T)}\right)_{T=T_g} \tag{10}$$

where m is the fragility index. The fragility index for 3VAc is found to be 63 at its T_g, whereas the reported value of the fragility index of PVAc is 96 [13]. It has been shown using data from more than 70 LMW glass formers and polymers that the non-Debye behavior (which can be realized in terms of increasing deviations of β_{KWW} from unity) of molecular dynamics is correlated with its fragility through the fragility index m [26]. At the respective T_g's, the β_{KWW} values for

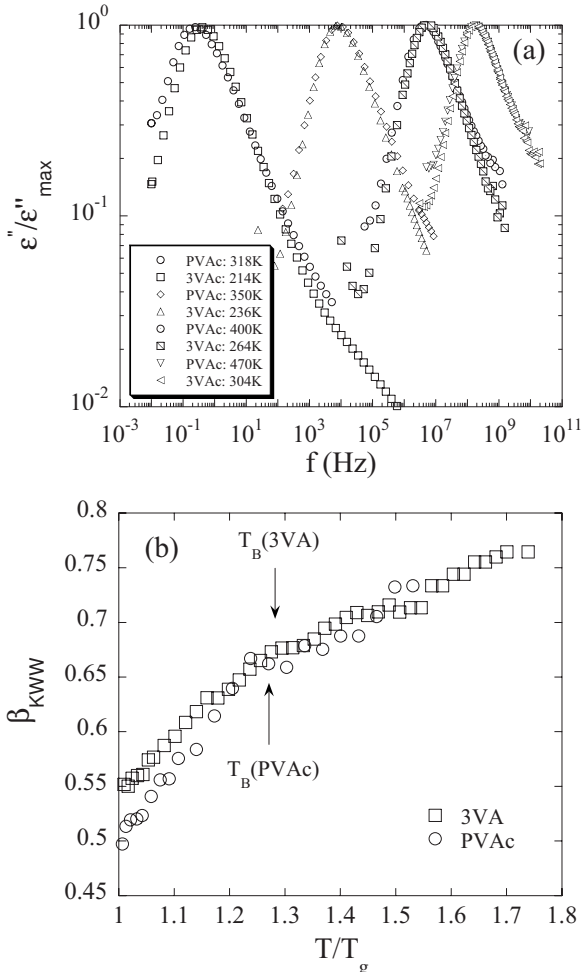

FIG. 6. (a) Log-log $\{\log_{10}\epsilon''$ vs $\log_{10}[f(\mathrm{Hz})]\}$ plot of normalized dielectric loss for 3VAc and PVAc at different temperatures. (b) Temperature variation of shape parameter β_{KWW} for 3VAc (squares) plotted against T/T_g. The corresponding data for PVAc have been taken from Ref. [13] for comparison.

3VAc and PVAc are 0.55 and 0.49. These values appear to be in agreement with the idea of increasing Debye behavior with decreasing fragility index. As a matter of fact, the fragility index for both PVAc and 3VAc could be given by the master equation $m=250(\pm 30)-320\beta$ proposed in Ref. [29]. Interestingly, if one considers only the high-temperature side of the diagram, PVAc seems to become stronger than its short-chain analog as PVAc shows less curvature of $\tau(T)$ for temperatures roughly above T_B (Fig. 5). Thus, the chain connectivity seems to be hardly correlated with the fragility.

Another interesting insight into the dynamics emerges from the comparison of the spectral shapes. For a direct comparison of the spectral shape, we have shown in Fig. 6(a) spectra of PVAc and 3VAc at different temperatures where the f_m is approximately the same. The PVAc spectrum looks slightly broader than the trimer near T_g. However, at the higher-T side it can be seen without any data analysis that around the α-relaxation peak the two curves overlap. Some deviations can be seen on the high-f side, which could be due to either the uncertainties in the weaker signal of PVAc or the T dependence of the high-frequency deviations. The same observation can be made quantitatively through the temperature variation of the HN shape parameter α or β_{KWW} parameter in the two cases [Fig. 6(b)]. Now, for the fitting procedure, as can be seen in Fig. 6(a) the deviations on the high-frequency side are rather similar in both systems and, hence, will influence the results less if the frequency range for the fitting is chosen carefully. In order to make sure that the fitting procedure is not affected by the high-frequency deviations, we have chosen a similar frequency range around the peak loss in both cases, and hence the resulting shape parameter should not be affected much. As we mentioned in Sec. III, the parameter α is the only shape parameter in fitting the HN equation. In our temperature window, the value of α changes from 0.823 ($T=209$ K) to 0.954 ($T=360$ K). The T dependence of the α parameter is very similar to the one obtained for β_{KWW}. However, for the sake of comparison of our results with the polymer counterpart we will stick to the β_{KWW} parameter obtained using Eqs. (3) and (4) in the following discussion. The strong temperature dependence of β_{KWW} in the case of 3VAc looks standard as, usually, simple glass formers show strong T dependence of the spectral shape. A direct comparison of β_{KWW} in the two cases reveals that β_{KWW} for PVAc is just a reflection of its LMW analog once the difference in T_g has been taken into account, which is surprising, particularly in view of the high values shown by PVAc on the high-T side. In polymers, usually, standard high-T asymptotic behavior of β_{KWW} (close to the value of 0.5) is observed, which is also compatible with the Rouse dynamics, where chain conformations are assumed to be Gaussian in nature [27]. The higher values of β_{KWW} found in the case of PVAc might suggest the decoupling of side group motions (where most of the dipolar bonds are located) from the main chain motions. In other words, the fluctuations in dipole moment perpendicular to the main chain (which are observed in a dielectric experiment on a polymeric system) could be influenced by side group motions that are usually coupled with α relaxation in the low-T regime but may occur rather independently at higher temperature. This could explain simultaneously the similar values of β_{KWW} in the polymer and 3VAc as, once the dipolar units become decoupled, the chain connectivity will be less relevant, and also our earlier finding that the dielectric relaxation times of PVAc are longer than the ones determined for the main chain dynamics by NMR [13].

The phenomenological description of the dielectric data also provides an important parameter, the dielectric strength $\Delta\epsilon$ $(=\epsilon_0-\epsilon_\infty)$ of the sample. An interesting aspect of chain connectivity on the dielectric properties can be seen through the comparison of $\Delta\epsilon$ at the T_g's. The $\Delta\epsilon$ values for 3VAc and PVAc at temperatures close to T_g are 9.1 and 6.3, respectively. The lower value found in the case of PVAc could be a direct consequence of its chain connectivity, as, usually, in polymers only the component of the dipole moment perpendicular to the main chain contributes to the observed dielectric strength. Let us now focus on the T dependence of the $\Delta\epsilon$. In a typical glass former, the $\Delta\epsilon$ usually decreases with increasing temperature as is depicted in Fig. 7. The results of PVAc have also been added in the same figure. The temperature variation of dielectric strength could be modeled according to the Onsager-Kirkwood-Frohlich theory [10,28], which

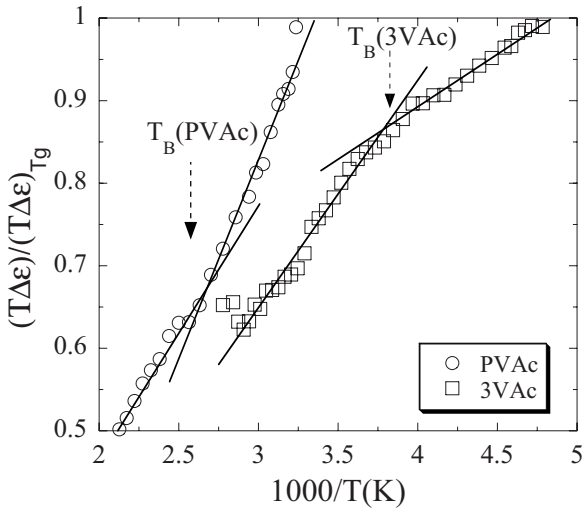

FIG. 7. Temperature variation of $T\Delta\epsilon$ (normalized to $T\Delta\epsilon$ at T_g) for 3VAc (squares) and PVAc (circles). Lines through the points are guides to the eye.

takes into account the modification of the dipole moment of a molecule inside a spherical cavity. The dielectric strength could then be given as

$$\epsilon_0 - \epsilon_\infty = \frac{\epsilon_0(\epsilon_\infty + 2)^2 g\mu^2 N}{9(2\epsilon_0 + \epsilon_\infty)k_B TV}, \tag{11}$$

where μ is the dipole moment of each unit, N is the total number of dipolar units, V is the volume, and g is a parameter quantifying the interactions between neighboring dipoles. Unfortunately, the unavailability of density data for the 3VAc sample prevented us from calculating absolute values of g. Nevertheless, with the available information the temperature variation of interaction parameter g could be considered. Assuming g to be T independent, the change in normalized values of $T\Delta\epsilon$ from 1 to 0.6 (Fig. 7) would correspond to a change of 40% in density in our temperature window of about 150 K. This is far too strong a T dependence for the density to be realized (most LMW glass formers and polymers show around 10–15 % of change in density in this temperature range [29]) and hence it is clear that the parameter g has to have strong T dependence and is decreasing with increasing temperature in this temperature range. It can also be seen that there is a slight change in the T dependence of $T\Delta\epsilon$ around T_B which could be yet another reflection of crossover in the values of g around T_B as was found in the case of PVAc [13] and other glass formers [30]. The change in T dependence of $\Delta\epsilon$ at T_B also hints at a change in the way the dipolar unit contributes to the observed dielectric strength. The origin of this change could be related to the existence of clustering, which is already well established near the glass transitions in many systems including PVAc [31,32]. One expects that this cluster structure would disappear as the temperature increases and the dynamics becomes more and more homogeneous in character.

B. β process

The β relaxation is considered an inherent part of the glassy dynamics and, therefore, its understanding can be very important to clarify the phenomenon of the glass transition. This is one of the reasons why the molecular origin of secondary relaxations has been debated extensively in the literature [33–35]. As mentioned briefly in Sec. IV, in our dielectric window a weak β process of 3VAc was observed below T_g. The characteristic times for this β process have been depicted in Fig. 4; they show simple Arrhenius behavior and can be fitted to Eq. (7) with the following characteristic parameters: $\tau_{0,\beta}=10^{-13.9}$ s and $E=39.9$ kJ/mol. The preexponential factor found in this case is of the order of typical vibrational frequencies. The β process of PVAc has been investigated by many authors [36–38] in the literature, although there exists some discrepancy between the reported relaxation rates. The temperature dependence of the relaxation rates from this work is also shown in Fig. 4 and fitted with the Arrhenius equation with the following parameters: $\tau_{0,\beta}=10^{-13.3}$ s and $E=40.4$ kJ/mol. Although, the preexponential factor is slightly higher than what is found in the case of 3VAc the activation energies of β processes in both cases are found to be the same within uncertainties. These results support the idea that secondary relaxations in these cases involve noncooperative and mainly intramolecular motions. On the other hand, the temperature variation of $\Delta\epsilon$ could be parametrized with $\Delta\epsilon_\beta(T)=\Delta\epsilon_\beta(T_g)[1+a_T(T-T_g)]$. The $\Delta\epsilon$ values at the respective T_g's for 3VAc and PVAc were found to be 0.175 and 0.095 (linear extrapolation). The temperature coefficient a_T of 3VAc was found to show a higher value of 3.4×10^{-3} in comparison to 9.1×10^{-4} for PVAc.

Let us now discuss the shape of the β processes. Usually, the β relaxations in molecular glasses are associated with local motions within the amorphous phase of the materials. The broadness of the β relaxations is, then, ascribed to the broad distribution of relaxation times in the frozen glassy state. This broadness of the relaxation spectra is expected to decrease as one goes higher in temperature, which should be reflected as an increase in the α_{CC} parameter. In a simple approach, by considering a Gaussian distribution of energy barriers, Eq. (7) yields a log-Gaussian distribution of relaxation times, each assumed to be an individual Debye process. In this approach, the full width at half maximum (FWHM) of the log-Gaussian distribution, σ is given as $\sigma=\sigma_E \log e/k_B T$, where σ_E^2 represents the variance of the corresponding distribution of energy barriers. Surprisingly, as can be seen in Fig. 8, the shape parameter of the β process in 3VAc remains essentially constant in our temperature window [39]. In other words, the distribution of relaxation rates remains the same within experimental uncertainty over the entire temperature range studied here.

On the contrary, when we move toward the polymer counterpart, we face a different situation, as the shape parameter increases monotonically with temperature, which results in a linear relationship of the σ parameter with the inverse of temperature. However, a finite value of σ at $T\to\infty$ is necessary to describe the relationship as

$$\sigma = \sigma_\infty + \frac{\sigma_E \log e}{k_B T}, \tag{12}$$

where σ_∞ is found to be close to 2.2 and σ_E has a value of 7 kJ/mole. The extrapolated value of σ exhibited for PVAc

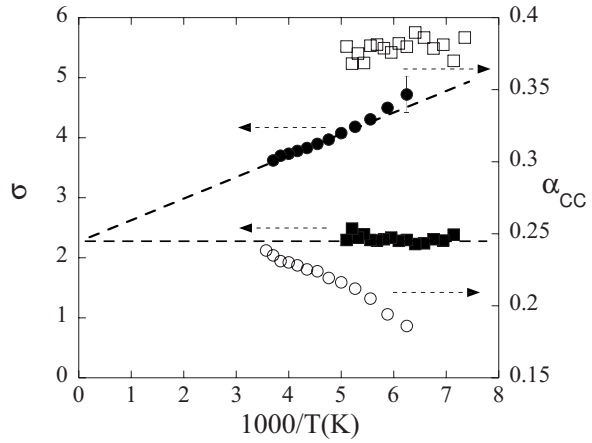

FIG. 8. Temperature variation of Cole-Cole shape parameter α_{CC} and σ parameter (width of log-Gaussian distribution) for secondary relaxations in 3VAc (squares) and PVAc (circle). The empty and filled symbols correspond to α_{CC} and σ parameters, respectively.

on the higher-T side (i.e., σ_∞) seems to merge with the temperature-independent value of σ for 3VAc. This could imply that the distribution of relaxation times for the β process of PVAc has two different contributions. One of the contributions is the same as the one found for 3VAc, and the other is associated with a distribution of energy barriers for the local molecular jumps responsible for such a process, the latter being about 16% (7 kJ/mole) according to our results. Thus, the comparison between 3VAc and the polymer suggests that in the latter case the origin of the distribution of activation energies is directly related to the chain connectivity. One explanation for this finding could be the possible small distortions of the covalent bond angles in the glassy polymer associated with chain connectivity, which would modify the energetically more favorable situation. Whether this extra contribution of chain connectivity to the distribution of relaxation times is a general feature remains open, because of the lack of a detailed comparison concerning this aspect in other systems.

On the other hand, an intriguing point which will need further investigation is the origin of the T-independent distribution of β-relaxation times found in 3VAc (contributing to PVAc as well). According to the Arrhenius equation, this finding suggests that the pre-exponential factor has a significant distribution (FWHM of nearly two decades). Finding an explanation for this experimental fact is not easy, as the distribution is too broad to be assigned only to a distribution of vibrational frequencies. One alternative approach could be to consider the Eyring equation [40], where the activation entropy (ΔS) is also considered as

$$\tau_{0,\beta} \approx \frac{h}{k_B T} \exp\left(\frac{-\Delta S}{R}\right), \tag{13}$$

so that it reduces to an Arrhenius-like equation when the activation entropy vanishes. In this framework, the distribution of the preexponential factor in the Arrhenius equation would be associated with a distribution of the activation entropy, which could be related to the number of particles participating in the molecular rearrangement.

VI. CONCLUSIONS

We have used broadband dielectric spectroscopy to investigate the dynamics of the short-chain analog of PVAc over a broad temperature range to cover the temperatures above and below T_g of 3VAc. The dielectric spectra for α relaxation were analyzed in terms of the Kolhraush-Williams-Watts model. A careful examination of the temperature dependence of the characteristic relaxation parameters indicates a crossover in dynamics at 261 K. This crossover temperature cannot be identified as the apparent merging temperature of α and β processes. The β process observed below the glass transition was found to be narrower than PVAc but showed the same activation energy of 40 kJ/mol. The direct comparison of the dynamics of PVAc with its short-chain analog showed interesting effects of chain connectivity. (i) It seems that the chain connectivity makes the dynamic crossover in relaxation rates weaker or less evident. (ii) Surprisingly, in this particular case no significant effects of connectivity were observed on the dielectric spectral shape in the high-T side. (iii) The β relaxation of PVAc shows an additional degree of heterogeneity, which could be related to a possible bond angle distribution in side chains.

ACKNOWLEDGMENTS

The authors acknowledge the University of Basque Country and Basque Country Government (Project No. 9/UPV00206.215-13568/2001) and the Spanish Ministry of Education (Project No. 2004-01017) for their support. The support of Donostia International Physics center is also acknowledged.

[1] J. Wong and C. A. Angell, *Glass Structure: By Spectroscopy* (Marcel Dekker, New York, 1976).
[2] *Broadband Dielectric Spectroscopy*, edited by F. Kremer and A. Schönhals (Springer-Verlag, Heidelberg 2003).
[3] S. S. N. Murthy, J. Phys. Chem. B **100**, 8508 (1996).
[4] F. Stickel, E. W. Fischer, and R. Richert, J. Chem. Phys. **102**, 6251 (1995).
[5] G. Williams and D. C. Watts, Trans. Faraday Soc. **66**, 80 (1970).
[6] A. Alegría, E. G. Echevarría, L. Goitiandía, I. Tellería, and J. Colmenero, Macromolecules **28**, 1516 (1995).
[7] J. Mattsson, R. Bergman, P. Jacobsson, and L. Börjesson, Phys. Rev. Lett. **94**, 165701 (2005).
[8] J. Mattsson, R. Bergman, P. Jacobsson, and L. Börjesson, Phys. Rev. Lett. **90**, 075702 (2003).
[9] C. Leon, K. L. Ngai, and C. M. Roland, J. Chem. Phys. **110**,

11585 1999.
[10] *Anelastic and Dielectric Effects in Polymer Solids*, edited by N. G. McCrum, B. E. Read, and G. Williams (Dover Publications, New York, 1967).
[11] S. Mashimo, R. Nozaki, S. Yagihara, and S. Takeishi, J. Chem. Phys. **77**, 6259 (1982).
[12] C. M. Roland and R. Casalini, Macromolecules **36**, 1361 (2003).
[13] M. Tyagi, A. Alegria, and J. Colmenero, J. Chem. Phys. **122**, 244909 (2005).
[14] Y. Miyake and T. Kominami, J. Chem. Soc. Jpn., Ind. Chem. Sect. **60**, 1340 (1957).
[15] E. Ikada, K. Shounaka, and M. Ashida, Polym. J. (Tokyo, Jpn.) **13**, 413 (1981).
[16] S. Havriliak and S. Negami, Polym. Lett. **14**, 99 (1966).
[17] F. Alvarez, A. Alegría, and J. Colmenero, Phys. Rev. B **44**, 7306 (1991).
[18] F. Alvarez, A. Alegría, and J. Colmenero, Phys. Rev. B **47**, 125 (1993).
[19] P. K. Dixon, L. Wu, S. R. Nagel, B. D. Williams, and J. P. Carini, Phys. Rev. Lett. **65**, 1108 (1990).
[20] C. A. Angell, J. Non-Cryst. Solids **131–133**, 13 (1991).
[21] M. H. Cohen and D. Turnbull, J. Chem. Phys. **31**, 1164 (1959).
[22] G. Adam and J. H. Gibbs, J. Chem. Phys. **43**, 139 (1963).
[23] R. Richert, Physica A **287**, 26 (2000).
[24] M. Paluch, R. Casalini, and C. M. Roland, Phys. Rev. E **67**, 021508 (2003).
[25] The corresponding parameters for the two VFT laws in the case of PVAc with appropriate temperature ranges are (1) low-T VFT (T range 309–360 K); $\log \tau_0 = -13.2$, $D = 7.4$, and $T_0 = 254.0$ K; (2) high-T VFT (T range 410–470 K); $\log \tau_0 = -11.8$, $D = 4.3$, and $T_0 = 280.5$ K.
[26] R. Böhmer, K. L. Ngai, C. A. Angell, and D. J. Plazek, J. Chem. Phys. **99**, 4201 (1993).
[27] D. Richter, M. Monkenbusch, A. Arbe, and J. Colmenero, *Neutron Spin Echo Investigations on Polymer Dynamics*; Advances in Polymer Science Vol. 174 (Springer-Verlag, Berlin, 2005).
[28] C. J. F. Böttcher, *Theory of Electric Polarization* (Elsevier Scientific, Amsterdam, 1973).
[29] *Physical Properties of Polymers Handbook*, edited by J. E. Mark (AIP, Woodbury, NY, 1996).
[30] A. Schönhals, Europhys. Lett. **56**, 815 (2001).
[31] K. Schmidt-Rohr and H. W. Spiess, Phys. Rev. Lett. **66**, 3020 (1991).
[32] U. Tracht, M. Wilhelm, A. Heuer, H. Feng, K. Schmidt-Rohr, and H. W. Spiess, Phys. Rev. Lett. **81**, 2727 (1998).
[33] G. P. Johari and M. Goldstein, J. Chem. Phys. **53**, 2372 (1970).
[34] M. Tyagi and S. S. N. Murthy, J. Chem. Phys. **114**, 3640 (2001).
[35] S. S. N. Murthy, J. Chem. Phys. **100**, 4601 (1994).
[36] K. Hikichi and J. Furuichi, Rep. Prog. Polym. Phys. Jpn. **4**, 69 (1961).
[37] Y. Ishida, M. Matsuo, and K. Yamafuji, Kolloid Z. Z. Polym. **180**, 108 (1962).
[38] D. Gomez, A. Alegría, A. Arbe, and J. Colmenero, Macromolecules **34**, 503 (2001).
[39] The CC shape parameter α_{CC} can be converted to the σ parameter by the following relationship: $\sigma = 10^{-3}/\alpha_{CC}^4 - 5.38 \times \log(\alpha_{CC})$.
[40] S. K. Glasstone, J. Laidler, and H. Eyring, *Theory of Rate Processes* (McGraw-Hill, New York, 1941), Chap. 10.